

pretations regarding the development of the mixing layer may be drawn based solely on centerline data. In particular, the growth rate and streamwise development of peak Reynolds stresses in the near field can be affected significantly by spanwise variations in the mixing layer. It is proposed here that some of the discrepancies in the past regarding growth rates and approach to self-similarity may have been caused by the lack of spanwise averaging. It is particularly important to employ spanwise averaging when comparing the development of mixing layers with different initial and operating conditions.

### Acknowledgments

This research was supported by NASA Grant NCC-2-55 from the Fluid Dynamics Research Branch, NASA Ames Research Center, and a National Science Foundation Grant NSF-MSM-88-15670.

### References

- <sup>1</sup>Brown, G. L., and Roshko, A., "On Density Effects and Large Structure in Turbulent Mixing Layers," *Journal of Fluid Mechanics*, Vol. 64, Pt. 4, 1974, pp. 775-816.
- <sup>2</sup>Lasheras, J. C., Cho., J. S., and Maxworthy, T., "On the Origin and Evolution of Streamwise Vortical Structures in a Plane, Free Shear Layer," *Journal of Fluid Mechanics*, Vol. 172, 1986, pp. 231-258.
- <sup>3</sup>Bell, J. H., and Mehta, R. D., "Three-Dimensional Structure of Plane Mixing Layers," Dept. of Aeronautics and Astronautics, Stanford Univ., Stanford, CA, JIAA TR-90, March 1989.
- <sup>4</sup>Bell, J. H., and Mehta, R. D., "Development of a Two-Stream Mixing Layer From Tripped and Untripped Boundary Layers," *AIAA Journal*, Vol. 28, No. 12, 1990, pp. 2034-2042.

## Approximate Formula of Weak Oblique Shock Wave Angle

Hua-Shu Dou\* and Hsueh-Ying Teng†  
Beijing University of Aeronautics and Astronautics,  
Beijing, People's Republic of China

### Introduction

**I**N the theory of oblique shock waves, the deflection angle  $\theta$  of flow across an oblique shock is related to the wave angle  $\beta$  by Eq. (1)<sup>1-3</sup>:

$$\frac{\tan(\beta - \theta)}{\tan\beta} = \frac{(\gamma - 1)M_1^2 \sin^2\beta + 2}{(\gamma + 1)M_1^2 \sin^2\beta} \quad (1)$$

For given upstream Mach number  $M_1$ , this is an implicit relation between  $\theta$  and  $\beta$ . With some trigonometric substitutions and rearrangement, Eq. (1) can be cast explicitly for  $\theta$  as

$$\tan\theta = \frac{2 \cot\beta(M_1^2 \sin^2\beta - 1)}{M_1^2(\gamma + \cos 2\beta) + 2} \quad (2)$$

which gives  $\theta$  as an explicit function of  $M_1$  and  $\beta$ .

In many problems with weak shocks determined by the deflection direction of flow (as shown in Fig. 1), the evaluation of the wave angle  $\beta$  in terms of the values of  $\theta$  and  $M_1$  is often required. This is commonly obtained from the charts related to Eq. (1), which can be inconvenient. Therefore, it is of significance to give an expression that formulates  $\beta$  as an explicit function of  $M_1$  and  $\theta$  for weak shock waves.

We encountered this problem in the research subject of shock wave/turbulent boundary-layer interactions and derived an approximate formula to evaluate  $\beta$  with the values of  $\theta$  and  $M_1$ .

### Derivation of Equations

When we rearrange Eq. (1), the following equation may be solved:

$$M_1^2 \sin^2\beta - 1 = \frac{\gamma + 1}{2} M_1^2 \frac{\sin\beta \sin\theta}{\cos(\beta - \theta)} \quad (3)$$

For small deflection angle  $\theta$ , Eq. (3) may be approximated by the following equation as that in Ref. 1

$$M_1^2 \sin^2\beta - 1 \approx \left( \frac{\gamma + 1}{2} M_1^2 \tan\beta \right) \theta \quad (4)$$

When  $\theta$  is small, the wave angle  $\beta$  approaches  $\pi/2$  for strong waves of Mach number  $M_2 < 1$  or goes to the Mach angle  $\mu$  for weak waves of Mach number  $M_2 > 1$ . Only the latter case is considered here. Therefore, when  $\theta = 0$ , the wave angle is equal to the Mach angle

$$\tan\beta = \tan\mu = \frac{1}{\sqrt{M_1^2 - 1}} \quad (5)$$

Using trigonometric identities,

$$\sin^2\beta = \frac{\tan^2\beta}{1 + \tan^2\beta} \quad (6)$$

Equation (4) may be then written as

$$\tan^2\beta = \frac{1}{M_1^2 - 1} + \frac{\gamma + 1}{2} \frac{M_1^2}{M_1^2 - 1} (\tan\beta + \tan^3\beta)\theta \quad (7)$$

Because of  $\theta \ll 1$  for the considered range of deflection angle  $\theta$ , we can assume a polynomial for  $\tan\beta$  in terms of the angle  $\theta$

$$\tan\beta = a + b\theta + c\theta^2 + \dots \quad (8)$$

where constants  $a$ ,  $b$ , and  $c$  are the functions of  $M_1$  only. Thus,

$$\tan^2\beta = a^2 + 2ab\theta + (2ac + b^2)\theta^2 + \dots \quad (9)$$

$$\tan^3\beta = a^3 + 3a^2b\theta + (3ab^2 + 3a^2c)\theta^2 + \dots \quad (10)$$

Substituting Eqs. (8) and (10) into Eq. (7), we have

$$\begin{aligned} \tan^2\beta = & \frac{1}{M_1^2 - 1} + \frac{\gamma + 1}{2} \frac{M_1^2}{M_1^2 - 1} [(a^3 + a) + (3a^2b + b)\theta \\ & + (3ab^2 + 3a^2c + c)\theta^2 + \dots] \theta \end{aligned} \quad (11)$$

Comparing Eqs. (9) and (11), we obtain

$$a = \frac{1}{\sqrt{M_1^2 - 1}} \quad (12a)$$

$$b = \frac{\gamma + 1}{4} \frac{M_1^4}{(M_1^2 - 1)^2} \quad (12b)$$

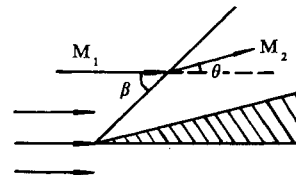


Fig. 1 Flow through an oblique shock wave.

Received Jan. 4, 1991; revision received May 20, 1991; accepted for publication May 20, 1991. Copyright © 1991 by the American Institute of Aeronautics and Astronautics, Inc. All rights reserved.

\*Lecturer and Candidate for Ph.D., Fluid Mechanics Institute.

†Professor, Fluid Mechanics Institute.

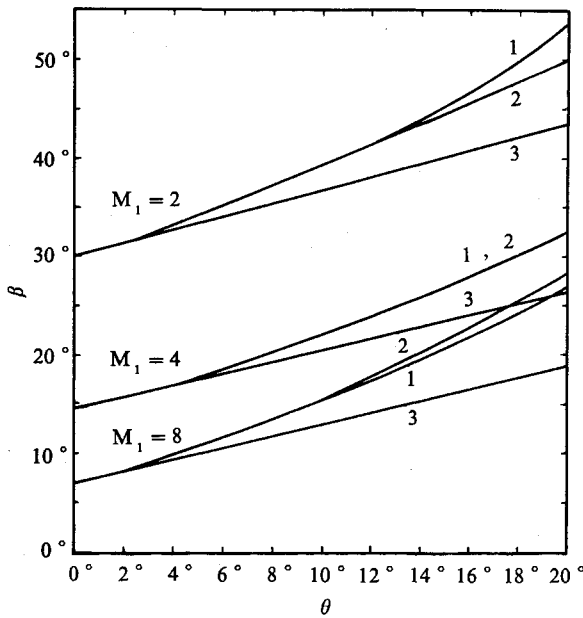


Fig. 2 Comparison of Eqs. (13) and (14) with Eq. (1): 1—accurate values [Eq. (1)]; 2—Eq. (13); 3—Eq. (14).

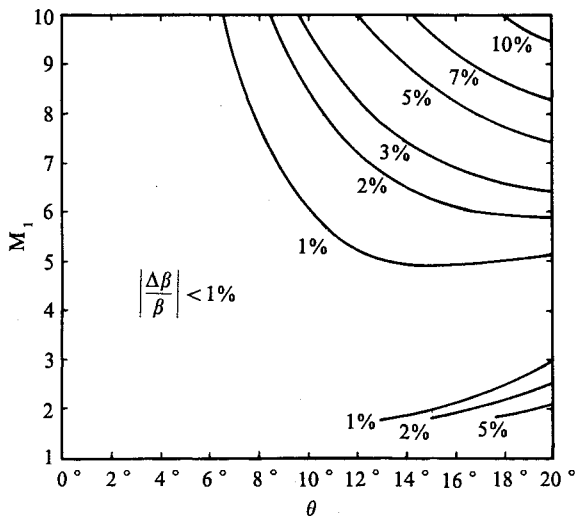


Fig. 3 Relative error isoline of Eq. (13) to Eq. (1).

$$c = \frac{1}{2} \left( \frac{\gamma + 1}{4} \right)^2 \frac{M_1^6 (M_1^2 + 4)}{(M_1^2 - 1)^{3.5}} \quad (12c)$$

Introducing Eqs. (12) into Eq. (8), and only taking the former three terms, it becomes

$$\tan \beta = \frac{1}{\sqrt{M_1^2 - 1}} + \frac{\gamma + 1}{4} \frac{M_1^4}{(M_1^2 - 1)^2} \theta + \frac{1}{2} \left( \frac{\gamma + 1}{4} \right)^2 \frac{M_1^6 (M_1^2 + 4)}{(M_1^2 - 1)^{3.5}} \theta^2 \quad (13)$$

Equation (13) is the approximate formula for evaluating the wave angle of weak shock waves. Using this equation, the value of  $\beta$  may be calculated easily for given  $M_1$  and  $\theta$ .

When  $\theta$  is very small, Eq. (13) can be simplified further,

$$\tan \beta = \frac{1}{\sqrt{M_1^2 - 1}} + \frac{\gamma + 1}{4} \frac{M_1^4}{(M_1^2 - 1)^2} \theta \quad (14)$$

The deviation of the wave angle  $\beta$  from the Mach angle  $\mu$  may be calculated from the values of  $\beta$  and  $\mu$ , which could be

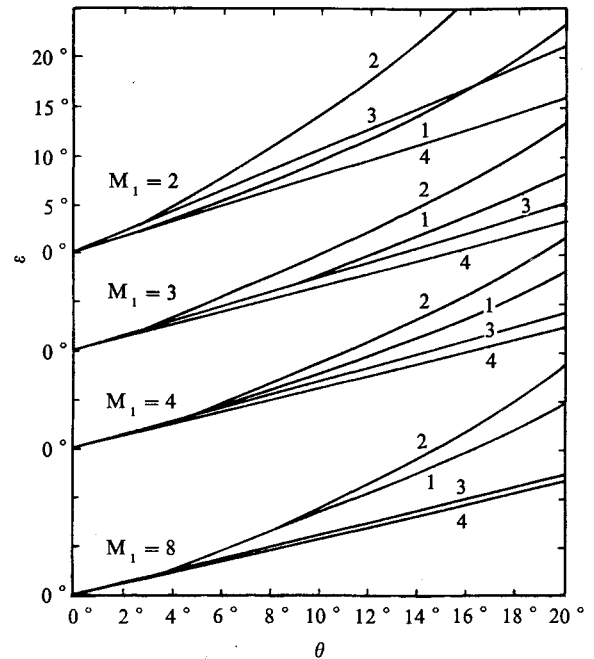


Fig. 4 Comparison of values of  $\epsilon$  angle: 1—accurate values [from Eqs. (15), (1), and (5)]; 2—Eq. (18); 3—Eq. (19); 4—Eq. (20).

obtained, respectively, from Eqs. (13) and (5). This also may be obtained with the approximate expression derived below. We may put

$$\beta = \mu + \epsilon \quad (15)$$

Because  $\epsilon \ll \mu$ ,  $\tan \epsilon \tan \mu \ll 1$ , therefore,

$$\begin{aligned} \tan \beta &= \tan(\mu + \epsilon) = \frac{\tan \mu + \tan \epsilon}{1 - \tan \mu \tan \epsilon} \doteq \tan \mu \\ &+ \tan \epsilon \doteq \tan \mu + \epsilon \end{aligned} \quad (16)$$

Rewriting Eq. (16),

$$\epsilon = \tan \beta - \tan \mu \quad (17)$$

Introducing Eqs. (13) and (5) into Eq. (17),

$$\epsilon = \frac{\gamma + 1}{4} \frac{M_1^4}{(M_1^2 - 1)^2} \theta + \frac{1}{2} \left( \frac{\gamma + 1}{4} \right)^2 \frac{M_1^6 (M_1^2 + 4)}{(M_1^2 - 1)^{3.5}} \theta^2 \quad (18)$$

When  $\theta$  is very small, we only take the linear form

$$\epsilon = \frac{\gamma + 1}{4} \frac{M_1^4}{(M_1^2 - 1)^2} \theta \quad (19)$$

For comparison, another approximate equation for  $\epsilon$  angle given in Ref. 1 is written as

$$\epsilon = \frac{\gamma + 1}{4} \frac{M_1^2}{M_1^2 - 1} \theta \quad (20)$$

## Results and Discussion

Calculated results using equations (1), (5), (13–15), and (18–20) are shown in Figs. 2–4 for a perfect gas, with  $\gamma = 1.40$ . It may be seen that Eq. (13) gives a satisfactory approximation of Eq. (1) for a wide range of  $M_1$  and a limited range of  $\theta$ . For  $\theta \leq 15$  deg and  $2 \leq M_1 \leq 7$ , the relative error is  $< 3\%$ . Figure 4 is the comparison of  $\epsilon$  values calculated with various equations. It is clear that Eq. (19) gives more accurate values than Eq. (20) for  $M_1 \geq 3$ .

Therefore, for weak shock waves, Eq. (13) can give  $\beta$  values that approach the accurate values over a wide range of  $M_1$  and  $\theta$ . With Eq. (13),  $\beta$  is evaluated easily from the values of  $\theta$  and  $M_1$ .

### References

- <sup>1</sup>Liepmann, H. W., and Roshko, A., *Elements of Gasdynamics*, Wiley, New York, 1957, pp. 84-93.
- <sup>2</sup>Anderson, J. D., Jr., *Fundamentals of Aerodynamics*, McGraw-Hill, New York, 1984, pp. 347-359.
- <sup>3</sup>Kuethe, A. M., and Chow, C. Y., *Foundations of Aerodynamics: Bases of Aerodynamic Design*, 4th ed., Wiley, New York, 1986, pp. 225-229.

## Using Rankine Vortices to Model Flow Around a Body of Revolution

B. S. Taylor\*

Portsmouth Polytechnic, Hampshire Terrace,  
Portsmouth, England, United Kingdom  
and

A. R. J. M. Lloyd†

Defense Research Agency, Haslar, Gosport,  
PO12 2AG, England, United Kingdom

### I. Introduction

IN Refs. 1 and 2, Lloyd described SUBSIM, a mathematical model to simulate deeply submerged maneuvers of a submarine. The model is based on a time-marching simulation of the changing flow around the maneuvering submarine and takes account of the vortices shed from the appendages and the separated flow on the hull. Similar techniques have been used to compute the maneuvering characteristics of missiles (see Ref. 3).

The flow around the submarine is described in terms of a distribution of shed vortices where the characteristics of the appendage vortices are computed using Glauert's<sup>4</sup> lifting-line theory while the vorticity shed from the hull is modeled using a total of 22 vortices. The positions and strengths of these are computed from empirical data measured on a submarine-like body of revolution (rounded nose and pointed tail) on the Rotating Arm facility at the Admiralty Research Establishment, Haslar, England, UK. The experiments were described by Lloyd and Campbell<sup>5</sup> and Lloyd.<sup>6</sup> They involved the direct measurement of vorticity using a Freestone probe<sup>7</sup> and the integration of vorticity contours to obtain circulation as a function of the body station, nondimensional turn rate, and drift velocity. Empirical equations fitted to the results are used to compute the strength and position of the hull vortices in SUBSIM.

Classical potential flow techniques are used to compute the velocities in planes transverse to the axis of the submarine. This allows the computation of the trajectories of the appendage vortices and also the calculation of the local incidence at various spanwise stations on each appendage. These local incidences are then used in the lifting-line calculations.

### II. Rankine Vortex

In the early development of the mathematical model, classical inviscid vortices were used with the velocity field given by

$$q = q_\psi \hat{\psi} = \frac{\Gamma}{2\pi R} \hat{\psi}$$

where  $\Gamma$  is the circulation,  $(R, \psi, z)$  refer to a system of cylindrical polar coordinates with the vortex at  $R = 0$ , and  $\hat{\psi}$  is a unit vector in the direction of increasing  $\psi$ .

The appropriate circulation of each vortex can be calculated, but the viscosity is zero everywhere except on the vortex filament itself where it is undefined. This is obviously not consistent with the experimental data. This approach also leads to the prediction of very large incidences when a vortex is close to an appendage.

For these reasons, it is more realistic to use the Rankine formulation

$$q = q_\psi \hat{\psi} = \frac{\Gamma}{2\pi R} [1 - \exp(-\alpha R^2)] \hat{\psi} \quad (1)$$

where  $\alpha$  is a constant. It is evident that this is equivalent to an inviscid vortex for large  $R$ , and since  $q = (\Gamma\alpha R)/2\pi$  for small  $R$ , the vortex behaves as if it has a solid core.

The core radius  $R_*$  is defined to be the radius at which maximum speed occurs, and so  $dq_\psi/dR = 0$  at  $R = R_*$ . From Eq. (1), it follows that  $2\alpha R_*^2 + 1 = \exp(\alpha R_*^2)$ , which gives the solution  $\alpha = 1.26/R_*^2$ .

The separated flow from the hull is modeled by a string of Rankine vortices. The circulation and core radius of each vortex is calculated from the experiment data. However, if the vortices are too far apart, they will retain their individual identity and produce discrete sets of nominally circular contours. We need to devise a test to establish whether the vortices will merge to produce continuous vorticity contours, representative of those measured in the experiment.

### III. Mathematical Condition for Merging

For two vortices of equal circulation and core radius at  $(D, 0)$  and  $(-D, 0)$ , the magnitude of the vorticity  $\zeta = \text{curl } \underline{q}$  at points on the  $x$  axis is given by

$$= \frac{1.26\Gamma}{\pi R_*^2} \left\{ \exp \left[ -1.26 \frac{(D-x)^2}{R_*^2} \right] + \exp \left[ -1.26 \frac{(D+x)^2}{R_*^2} \right] \right\}$$

relative to an origin midway between the vortices.

Putting  $y = x/D$  and  $s = R_*/D$ , this becomes

$$\zeta' = \frac{\pi D^2 \zeta s^2}{1.26\Gamma} = \left\{ \exp \left[ -1.26 \left( \frac{1-y}{s} \right)^2 \right] + \exp \left[ -1.26 \left( \frac{1+y}{s} \right)^2 \right] \right\}$$

The nondimensional vorticity  $\zeta'$  is plotted for various values of the nondimensional core radius in Fig. 1. It can be seen that for small values of the core radius the vorticity distribution indicates two distinct vortices. As the core radius increases, the vortices merge. Now,

$$\frac{d\zeta'}{dy} = \frac{2.52}{s^2} \left\{ (1-y) \exp \left[ -1.26 \left( \frac{1-y}{s} \right)^2 \right] - (1+y) \exp \left[ -1.26 \left( \frac{1+y}{s} \right)^2 \right] \right\}$$

The vorticity is a maximum (or minimum) when  $d\zeta'/dy = 0$  and this occurs when

$$\frac{1-y}{1+y} = \exp \left[ -5.04 \frac{y}{s^2} \right] \quad (2)$$

Received Dec. 17, 1990; revision received May 7, 1991; accepted for publication May 13, 1991. Copyright © 1991 by the American Institute of Aeronautics and Astronautics, Inc. All rights reserved.

\*Principal Lecturer.

†Principal Scientific Officer, Maritime Division.